

Dynamics of a turbojet engine considered as a quasi-static system

Constantin Rotaru, MihaiAndres-Mihăilă, Pericle Gabriel Matei and RalucaIoana Edu

Abstract—Turbojet engine dynamics arise from complex interacting phenomena: gas flow behavior in the compressor and turbine, shaft inertias and losses, fuel flow transport delay, combustion and thermal behavior of the engine and its surroundings. This paper presents a linearized mathematical model of a turbojet engine, based on the Taylor's series expansion of the torque function, which allows for the engine's dynamic characteristics study. The numerical solver used in the simulation packages relies on the rotor speed as one of the independent variables. Several approaches of the nonlinear characteristics of the engine model were considered to choose the methodology that better predicts the temperature field in the combustion chamber.

Keywords—aircraft engine, control system, dynamic model, Laplace transform, turbojet.

I. INTRODUCTION

THE turbojet engine represents one of the most efficient forms of propulsion and power generation, with applications ranging from land-based power generation, on board power and propulsion sources for marine ships, to aircraft propulsion systems. Design of such complex machinery requires the knowledge of multiple academic disciplines including mathematics, aerodynamics, fluid mechanics, solid mechanics, thermodynamics, chemistry and material sciences. An aircraft engine operates in a wide operating envelope (to support aircraft mission requirements). The operating envelope is typically defined as a graph of flight altitude vs flight Mach number [1].

Compatibility of pressure in adjacent components and core flow equality throughout the engine restrict the possible steady operating points and transient trajectories observed in a component map. Compressor maps are typically used as the common platform on which all constraints are represented. The engine operating line is the locus of compressor pressure ratio and mass flow rate points obtained at steady-state

conditions as an engine input is varied. In single-input controlsystems, fuel flow rate is changed by adjusting a throttle setting. The resulting compressor pressure ratio and air mass flow rate are plotted on the compressor map once a steady-state has been reached [2].

A gas turbine engine is inherently nonlinear as a result of the complex interactions of thermal, fluid, and mechanical effects. These nonlinear characteristics also appear in engine model. However, nonlinear models are typically not used in control law design because the characteristics of nonlinear models (or systems) change with the initial and the current operating conditions, making nonlinear design techniques too generalized for meeting specific performance requirements at a specific operating condition.

The fuel ratio unit has been accepted as the fuel control variable instead of the simpler fuel flow rate as the primary fuel control variable, because: the fuel ratio provides a good control of turbine gas temperature; it provides a self-recovery feature when the engine surge; it simplifies the control law by reducing the variability of the controller gain constant. The corrected fuel flow for the main burner depends on both the total pressure and the total temperature at the compressor inlet. By choosing the compressor exit static pressure as the correction parameter, it could be reduce the difference in fuel ratios between the take-off power and the idle power [3]. By reducing this ratio means to reduce the size of the fuel scheduling cam in the hydro-mechanical control unit. When the fuel ratio is used as the control variable, it needs to be multiplied by the compressor exit pressure to get the actual fuel flow rate that is injected in the combustion chamber. This logic is illustrated in the Fig. 1. This multiplication step ensures that the fuel flow rate going into the main burner is reduced when the engine starts to stall or surge. For some aviation applications, a gas turbine engine must provide a wide range of predictable and repeatable thrust performance over the entire operating envelope of the engine, which can cover the altitude from sea level to tens of thousands meters. These altitude changes along with variations in flight speed from takeoff to supersonic velocities result in large, simultaneous variations in engine inlet temperature, inlet pressure and exhaust pressure. These large variations in engine operating conditions and the demand for precise thrust control, coupled with the demand for highly reliable operations, despite the complexity of the engine itself, create a significant challenge for the design of the engine control systems [4].

Constantin Rotaru is with the Aviation Integrated Systems and Mechanics Department, Military Technical Academy, Bucharest, Romania (tel: +40745974488; fax: +4021 335 57 63; e-mail: rotaruconstantin@yahoo.com).

Mihai Andres-Mihăilă is with the Aviation Integrated Systems and Mechanics Department, Military Technical Academy, Bucharest, Romania (e-mail: mihailmi@rdslink.ro)

Pericle Gabriel Matei is with the Aviation Integrated Systems and Mechanics Department, Military Technical Academy, Bucharest, Romania (e-mail: pgmatei@yahoo.com).

RalucaIoanaEdu is with the Aviation Integrated Systems and Mechanics Department, Military Technical Academy, Bucharest, Romania (e-mail: edu_ioana_raluca@yahoo.com).

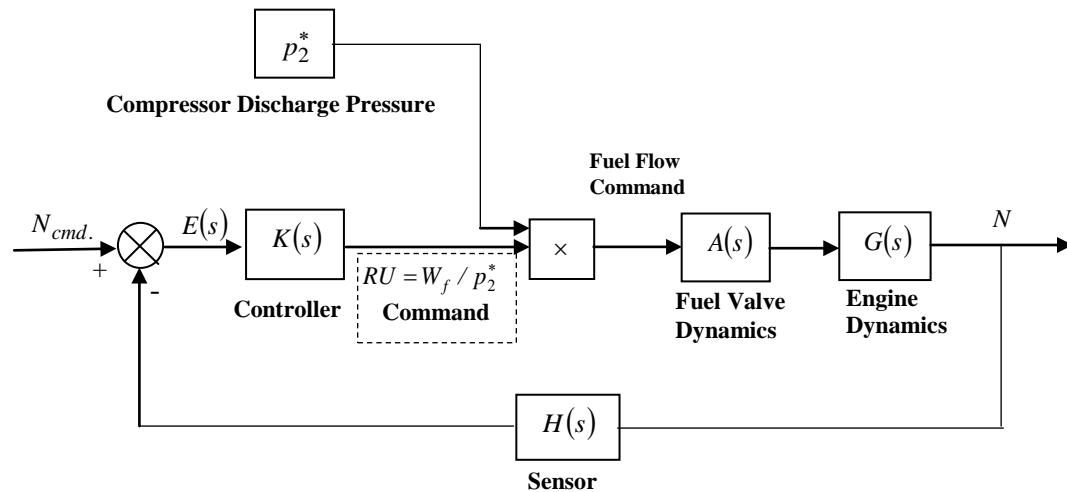


Fig. 1 Control logic relating controller output to main burner fuel flow rate

Control system complexity can be measured by the number of control variables or by the number of measured variables in the system. Typically, the number of control variables corresponds directly to the number of actuators and the number of measured variables to the number of sensors. The control variables could be: compressor inlet variable vane position command; rear compressor variable vane position command; compressor tip clearance control valve; cowl cooling control valve; main burner fuel valve; combustor mode valve; surge/variable bleed command; high pressure (HP) and low pressure (LP) turbine tip clearance control valve; fuel flow command; exhaust nozzle area command. Because measured variables are used to provide feedback to the control system, as well as to provide awareness of the health of the engine, the number of measured variables is also a good measure of control complexity [5]. The measured gas-patch variables could be: fan inlet total temperature; fan inlet or ambient pressure; compressor inlet temperature; compressor discharge temperature; burner pressure or compressor discharge pressure; compressor bleed pressure; high pressure turbine blade metal temperature; inter-turbine temperature; exhaust temperature; turbine exit total pressure (fan & core mixed stream); LP spool speed; HP spool speed.

II. COMPONENT MAP AND COMBUSTION MODEL

The thermal energy of the air/fuel mixture flowing through an air-breathing engine is increased by the combustion process. The fuel must be vaporized and mixed with the air before this chemical reaction can occur. Once this is done, the combustion process can occur and thus increase the thermal energy of the mixture.

The coordinates of a point in the compressor map correspond to steady-state operation at some mass flow rate and corresponding pressure ratio. Unique values of rotor speed and efficiency exist for a given set of compressor map coordinates.

Efficiency and speed data are represented in the map in the form of constant-efficiency and constant-speed lines. Specifically, the adiabatic efficiency of compression is used, given by the ratio of the work needed to raise the pressure under isentropic conditions to the actual work required to produce the same pressure ratio. If mass flow rate and pressure ratio are independently given, unique values exist for rotor speed and adiabatic efficiency.

Newton's law is readily applied to core and fan shafts, making their speeds a natural choice of state variables. Rotor speed, however, cannot be paired with mass flow rate, pressure ratio or efficiency to form a set of independent variables, more than one value of mass flow rate may correspond to a choice of pressure ratio and rotor speed [6].

Figure 2 shows such engine operating line and various constraints represented on a compressor map.

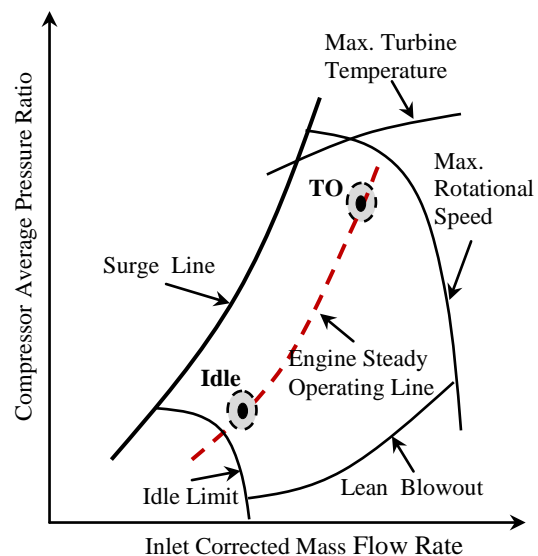


Fig. 2 Engine operating limits on compressor map

Heat release due to combustion and acoustic wave propagation are dynamically coupled phenomena and the characteristics of this interaction are modulated by the fuel flow rate imposed by the pump. Under normal operating conditions, variables such as combustor pressure and temperature exhibit stable responses to changes in fuel flow rate. If perturbations are introduced to a steady flow condition so that pressure and heat release are in phase, resonant oscillations are induced [7].

Lean blowout occurs when the air-to-fuel ratio is very small. This condition may be encountered upon sharp decelerations, when the control system commands a decrease in fuel flow rate (Fig. 3). Aircraft descent involves engine operation near idle speeds, which corresponds to minimal fuel flow rates. Each point in a compressor map corresponds to a combination of mass flow rate and pressure ratio. The locus of compressor map points having a fuel flow rate equal to the lean blowout can be represented as an additional operating boundary to be taken into account. Compressor maps are typically used as the common platform on which all constraints are represented. Figure 3 shows the engine operating line, where the compressor pressure ratio and mass flow rate points are obtained at steady-state conditions as an engine input is varied [8].

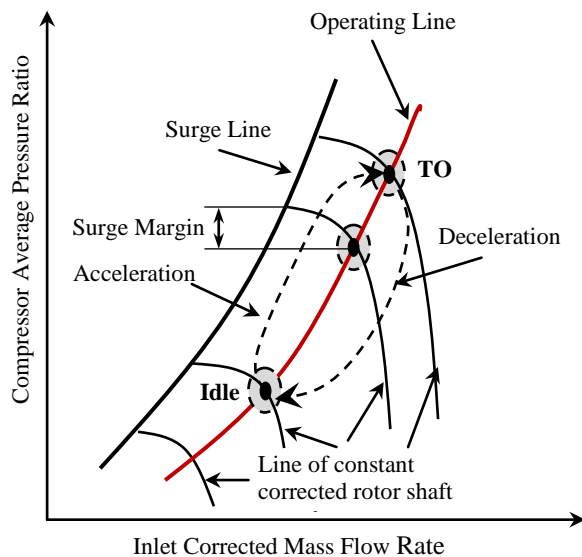


Fig. 3 Engine operating line on compressor map

The operating line can shift up or down on the compressor map depending on the amount of bleed air and shaft power extracted from the engine. Even if the operating line stays unchanged on the compressor map, a set point can move to the left or right along the operating line for the same throttle position, because the idle and take off (TO) power set points change with the altitude and inlet temperature, and because the exact fan speed or pressure ratio command for each set point is proportional to the difference between the corresponding commands at idle and TO [9].

A self-stabilized, steady flow combustion system requires

two distinct regions: a primary zone (well stirred reactor) in which the flow stream is recirculated in order to promote gross mixing of products, reactants and reaction intermediates (being governed by a coupled set of nonlinear equations) and a secondary zone (Fig. 4) which has the main function to allow sufficient convective residence time for the primary zone effluent to burn out before exiting the combustor (plug flow reactor).

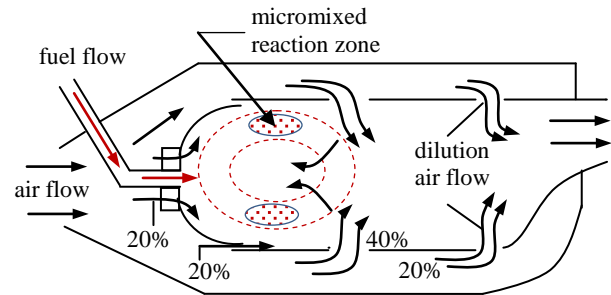


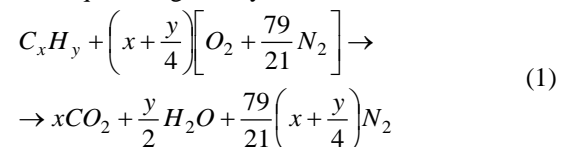
Fig. 4 Combustion chamber flow pattern

A typical distribution of airflow into a can-contained combustion zone is presented in the above figure, where about 20% of the intake air passes through swirling vanes that surround the central fuel spray nozzle. The primary zone in which the fuel-air ratio is nearly stoichiometric, is fed by other airflow (about 80%) [10]. These flows are designed to interact in such a way that a large and steady swirl is established in the primary combustion zone.

The rates of reaction in a turbojet combustion chamber are affected by both chemical kinetics and mixture turbulence which controls the rate of mixing of fuel and air, and also the instantaneous geometry of the flame surface. The flame travels into a mixture of reactants at a rate that is dependent on the state of the reactants and is limited either by mixture turbulence or by chemical kinetics.

A flame remains stationary in a traveling mixture of reactants if the speed of the flame relative to the reactants is just equal to the reactants mixture velocity. Turbulence can rise the burning velocity, so, the flame tube must have the zones of low velocity in which the flames can propagate into an unburned mixture.

The maximum combustion temperature occurs when hydrocarbon fuel molecules are mixed with just enough air, so that, all of the oxygen atoms are consumed, all of the hydrogen atoms form water vapor and all of the carbon atoms form carbon dioxide CO_2 . This ideal mixture of fuel and air is represented by a general atom balance equation, called the stoichiometric equation, given by



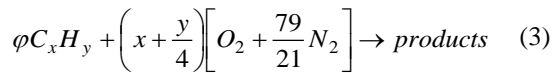
The stoichiometric mass-basis fuel/air ratio is

$$f_{st} = \frac{36x + y}{103(4x + y)} \quad (2)$$

Although the stoichiometric ratio for most fuels is typically 0.06 to 0.07 and the fuel-to-air ratio for the engine is 0.015 to 0.03, in the primary burning zone of the combustion chamber, the mixture is fuel rich and this ratio is typically 0.08 [9].

Because the overall performance of an engine and the life of the turbine, are strongly dependent on burner exit temperature, predicting this temperature is extremely important. All jet fuels are hydrocarbons and most of them have characteristics similar to those of kerosene.

The fuel/air equivalence ratio is defined as the ratio of the actual fuel/air ratio to the stoichiometric fuel/air ratio $\phi = f / f_{st}$ and it permits representation of either fuel-rich or fuel-lean mixtures by multiplying the fuel term in the atom-balance equation by ϕ



Ignition of a fuel/air mixture in a turbojet combustion system requires inlet air and fuel conditions within flammability limits, sufficient residence time of a combustible mixture and location of an effective ignition source in the vicinity of the combustible mixture.

When the temperature in the combustion system is below the spontaneous ignition temperature, an ignition source is required to bring the local temperature above the spontaneous ignition temperature.

III. DYNAMIC ENGINE MODELS

The acceleration of the rotor (consisting of the compressor, turbine and the shaft) based on the principle of Newtonian mechanics is

$$\dot{\omega} = \frac{\Delta M}{J} \quad (4)$$

where $\dot{\omega}$ is the angular acceleration of the rotor, $\Delta M = M_T - M_C$ represents the difference between the torque produced by the turbine, M_T , and the torque required by the compressor, M_C , and J is the mass moment of inertia of the compressor-shaft-turbine body (Fig. 5). The angular velocity ω is usually substituted by the shaft rotational speed N and the differential torque ΔM is represented by a function of shaft speed and fuel flow rate W_f . Substituting these in the torque function, the equation for the shaft rotational speed is expressed as

$$\dot{N} = \frac{f(N, W_f)}{J} \quad (5)$$

Engine dynamics arise from complex, interacting phenomena. Due to the intricate geometry of the engine components and the complexity of gas flow, algebraic expression for f is unavailable. This function is highly dependent on external variables such as aircraft speed and atmospheric conditions, which act as its parameters.

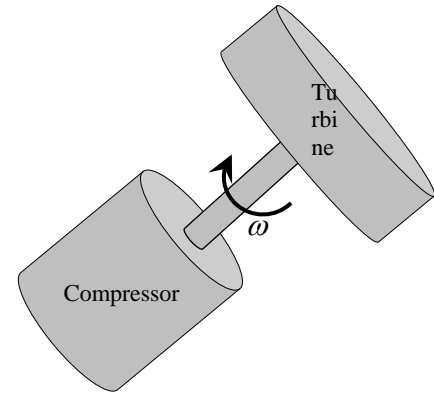


Fig. 5 Engine shaft dynamics

The linear model of shaft dynamics for one-spool engine, based on the Taylor's series expansion of the function f at a (steady-state) nominal operating point is

$$\dot{N} = \frac{1}{J} \frac{\partial f}{\partial N} \cdot \Delta N + \frac{1}{J} \frac{\partial f}{\partial W_f} \cdot \Delta W_f \quad (6)$$

The partial derivatives of f are obtained from a perturbation method based on experimental, collected from a host of sensors, from which relevant quantities such as adiabatic efficiencies and stall margins are computed. To obtain an approximate value of a partial derivative, the dependent variable is slightly perturbed from its steady value, and the corresponding increment in net torque recorded. While a controls-oriented model can be as simple as a single linear model corresponding to a point in the grid, a high-fidelity simulation model uses partial derivative information obtained from a fine grid covering the entire flight envelope [2].

The output equation for any engine variable y can be expressed as a function of speed and fuel flow as well, so that a small variation of the output variable from its nominal value is expressed as

$$y = \frac{\partial y}{\partial N} \cdot \Delta N + \frac{\partial y}{\partial W_f} \cdot \Delta W_f \quad (7)$$

The first order partial derivatives, similar to stability derivatives in airplane dynamics, are evaluated at the specific nominal condition, about which the linear model is expected to apply.

The transfer function from the input variable fuel flow to the output variable y is expressed as

$$\frac{Y(s)}{W_f(s)} = \frac{cb}{s-a} + d \quad (8)$$

where

$$a = \frac{1}{J} \frac{\partial M}{\partial N}; b = \frac{1}{J} \frac{\partial M}{\partial W_f}; c = \frac{\partial y}{\partial N}; d = \frac{\partial y}{\partial W_f}; \quad (9)$$

For a gas turbine engine, the coefficient a is always less than zero in the control envelope. Equation (8) represents a first-order lag, which means that the speed response behaves like a lag function after the fuel flow is changed.

The linear model of shaft dynamics for a two-spool jet engine can be derived by extending the one-spool model of

(6) and (7) with the dynamics of the second shaft. For a two-spool engine we have

$$\begin{cases} \dot{N}_1 = \frac{1}{J_1} \left(\frac{\partial M_1}{\partial N_1} \cdot \Delta N_1 + \frac{\partial M_1}{\partial N_2} \cdot \Delta N_2 + \frac{\partial M_1}{\partial W_f} \cdot \Delta W_f \right) \\ \dot{N}_2 = \frac{1}{J_2} \left(\frac{\partial M_2}{\partial N_1} \cdot \Delta N_1 + \frac{\partial M_2}{\partial N_2} \cdot \Delta N_2 + \frac{\partial M_2}{\partial W_f} \cdot \Delta W_f \right) \end{cases} \quad (10)$$

where

$$\begin{cases} \Delta M_1 = \dot{m}_{c1} c_{p_{c1}} (T_{4.1}^* - T_4^*) - \dot{m}_{c1} c_{p_{c1}} (T_{2.1}^* - T_1^*) \\ \Delta M_2 = \dot{m}_{c2} c_{p_{c2}} (T_3^* - T_{4.1}^*) - \dot{m}_{c2} c_{p_{c2}} (T_2^* - T_{2.1}^*) \end{cases} \quad (11)$$

Similarly, the output equation is given by

$$y = \frac{\partial y}{\partial N_1} \cdot \Delta N_1 + \frac{\partial y}{\partial N_2} \cdot \Delta N_2 + \frac{\partial y}{\partial W_f} \cdot \Delta W_f \quad (12)$$

In the matrix notation, the shaft dynamics for a tow-spool engine are expressed as

$$\begin{bmatrix} \dot{N}_1 \\ \dot{N}_2 \end{bmatrix} = \begin{bmatrix} a_{11} & a_{12} \\ a_{21} & a_{22} \end{bmatrix} \begin{bmatrix} N_1 \\ N_2 \end{bmatrix} + \begin{bmatrix} b_1 \\ b_2 \end{bmatrix} W_f \quad (13)$$

$$y = [c_1 \quad c_2] \begin{bmatrix} N_1 \\ N_2 \end{bmatrix} + [d] W_f \quad (14)$$

The frequency-domain representation of two-spool engine dynamics expressed in transfer function form for the output variable y is

$$\frac{Y(s)}{W_f(s)} = C(sI - A)^{-1} B + D = \frac{k(s + z_1)}{(s + r_1)(s + r_2)} \quad (15)$$

where I is the identify matrix. This transfer function represents a second-order dynamic system.

IV. NUMERICAL RESULTS

Starting from hypothesis that the compressor air flow rate, G_a , is equal to the turbine gas flow rate, G_{gT} , applying the energy and mass conservation theorems, one can get

$$\begin{cases} \frac{\pi J}{30} \frac{dN}{dt} = M_T - M_C \\ \frac{T_2^*}{T_1^*} = 1 + \left(\frac{\gamma-1}{\pi_C^* \gamma} - 1 \right) \frac{1}{\eta_C} \\ G_a = G_{gT} \\ \frac{T_4^*}{T_3^*} = 1 - \left(1 - \frac{1}{\pi_C^* \gamma'} \right) \eta_T^* \\ G_{gT} = G_{noz} \\ W_f H_u \eta_{ca} = c_p G_a (T_3^* - T_2^*) \end{cases} \quad (16)$$

where N is the rotational speed, J - inertia momentum, G - flow rate for air and gases (subscripts a, gT and noz), H_u - low heating value of fuel). After some simple transformations the above equations become:

$$\begin{cases} T^{(1)} \frac{d\bar{N}}{dt} + \rho^{(1)} \bar{N} - k_{T_3^*}^{(1)} \bar{T}_3^* + 0 \cdot \bar{T}_4^* - k_{p_2^*}^{(1)} \bar{p}_2^* + k_{p_4^*}^{(1)} \bar{p}_4^* = 0 \\ k_n^{(2)} \bar{N} - k_{T_3^*}^{(2)} \bar{T}_3^* + 0 \cdot \bar{T}_4^* + k_{p_2^*}^{(2)} \bar{p}_2^* + 0 \cdot \bar{p}_4^* = 0 \\ 0 \cdot \bar{N} - \bar{T}_3^* + \bar{T}_4^* - k_{p_2^*}^{(3)} \bar{p}_2^* - k_{p_4^*}^{(3)} \bar{p}_4^* = 0 \\ 0 \cdot \bar{N} + k_{T_3^*}^{(4)} \bar{T}_3^* - k_{T_4^*}^{(4)} \bar{T}_4^* + k_{p_2^*}^{(4)} \bar{p}_2^* - k_{p_4^*}^{(4)} \bar{p}_4^* = 0 \\ k_n^{(5)} \bar{N} + k_{T_3^*}^{(5)} \bar{T}_3^* + 0 \cdot \bar{T}_4^* + k_{p_2^*}^{(5)} \bar{p}_2^* + 0 \cdot \bar{p}_4^* = k_{G_c}^{(5)} \bar{W}_c \end{cases} \quad (17)$$

where

$$T^{(i)} = \frac{\pi J N_0}{30 M_0};$$

$$\rho^{(i)} = \frac{N_0}{M_0} \left[\left(\frac{\partial M_C}{\partial G_a} \right)_0 \left(\frac{\partial G_a}{\partial n} \right)_0 + \left(\frac{\partial M_C}{\partial n} \right)_0 - \left(\frac{\partial M_T}{\partial n} \right)_0 \right];$$

$$k_{T_3^*}^{(1)} = \frac{(T_3^*)_0}{M_0} \left[\left(\frac{\partial M_T}{\partial T_3^*} \right)_0 + \left(\frac{\partial M_T}{\partial G_{gT}} \right)_0 \left(\frac{\partial G_{gT}}{\partial T_3^*} \right)_0 \right];$$

$$k_{p_2^*}^{(1)} = \frac{(p_2^*)_0}{M_0} \left[\sigma_{ca} \left(\frac{\partial M_T}{\partial G_{gT}} \right)_0 \left(\frac{\partial G_{gT}}{\partial p_2^*} \right)_0 + \frac{\sigma_{ca}}{(p_4^*)_0} \left(\frac{\partial M_T}{\partial \pi_T^*} \right)_0 - \left(\frac{\partial M_C}{\partial G_a} \right)_0 \left(\frac{\partial G_a}{\partial \pi_C^*} \right)_0 \frac{1}{(p_1^*)_0} - \left(\frac{\partial M_C}{\partial \pi_C^*} \right)_0 \frac{1}{(p_1^*)_0} \right]$$

$$k_{p_4^*}^{(1)} = \frac{(\pi_T^*)_0}{M_0} \left(\frac{\partial M_T}{\partial \pi_T^*} \right)_0; \quad k_n^{(2)} = \frac{N_0}{(G_a)_0} \left(\frac{\partial G_a}{\partial n} \right)_0;$$

$$k_{p_2^*}^{(2)} = \frac{(p_2^*)_0}{(G_a)_0} \left[\left(\frac{\partial G_a}{\partial p_2^*} \right)_0 - \sigma_{ca} \left(\frac{\partial G_{gT}}{\partial p_3^*} \right)_0 \right];$$

$$k_{T_3^*}^{(2)} = \frac{(T_3^*)_0}{(G_{gT})_0} \left(\frac{\partial G_{gT}}{\partial T_3^*} \right)_0; \quad k_{p_2^*}^{(3)} = - \frac{\gamma_1}{(\pi_T^*)_0 (1 - \eta_T^*) + \eta_T^*};$$

$$k_{p_4^*}^{(3)} = \frac{\gamma_1}{(\pi_T^*)_0 (1 - \eta_T^*) + \eta_T^*}; \quad k_{T_3^*}^{(4)} = \frac{(T_3^*)_0}{(G_{gT})_0} \left(\frac{\partial G_{gT}}{\partial T_3^*} \right)_0;$$

$$k_{T_4^*}^{(4)} = \frac{(T_4^*)_0}{(G_{noz})_0} \left(\frac{\partial G_{noz}}{\partial T_4^*} \right)_0; \quad k_{p_2^*}^{(4)} = \frac{\sigma_{ca} (p_2^*)_0}{(G_{gT})_0} \left(\frac{\partial G_{gT}}{\partial p_3^*} \right)_0;$$

$$k_{p_4^*}^{(4)} = \frac{(p_4^*)_0}{(G_{noz})_0} \left(\frac{\partial G_{noz}}{\partial p_4^*} \right)_0; \quad k_{T_3^*}^{(5)} = \frac{c_p (T_3^*)_0 (G_a)_0}{Q_0};$$

$$k_n^{(5)} = \frac{c_p N_0 [(T_3^*)_0 - (T_2^*)_0]}{Q_0} \left(\frac{\partial G_a}{\partial n} \right)_0; \quad Q_0 = (W_f)_0 H_u \eta_{ca};$$

$$k_{p_2^*}^{(5)} = \frac{c_p}{Q_0} \left[\frac{(p_2^*)_0 [(T_3^*)_0 - (T_2^*)_0]}{\left(\frac{\partial p_2^*}{\partial p_2^*} \right)_0} - \frac{\gamma (T_2^*)_0 (G_a)_0 (\pi_C^*)_0}{(\pi_C^*)_0 \gamma + \eta_C^* - 1} \right];$$

$$k_{G_c}^{(5)} = \frac{(W_f)_0 H_u \eta_{ca}}{Q_0};$$

The station numbering and the nomenclature used in the above equations are presented at the end of the article.

The transfer function from the input variable fuel flow, $\bar{W}_f(s)$, to the output variable, $\bar{N}(s)$, for an one-spool engine with

$$G_a = 50 \text{ kg/s}; T_3^* = 1200 \text{ K}; \pi_c^* = 6; H_u = 42000 \text{ kJ/kg};$$

$$J = 4.3 \text{ kg} \cdot \text{m}^2; N_0 = 10000 \text{ rot/min}$$

is

$$\frac{\bar{N}(s)}{\bar{W}_f(s)} = \frac{1.64}{1.04s + 14.18} \quad (18)$$

The responses of the rotational speed $\bar{N}(t) = \Delta N / N_0$ to an impulse input (Dirac function), to a unit step input (Heaviside function) and to a sinusoidal input ($s = i\omega$) are presented in Figures 6, 7 and 8.

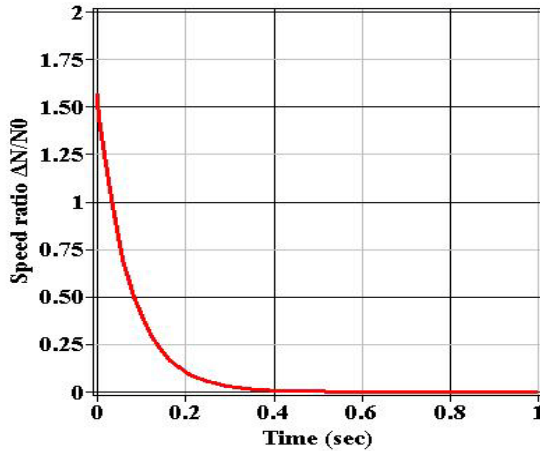


Fig. 6 Impulse response

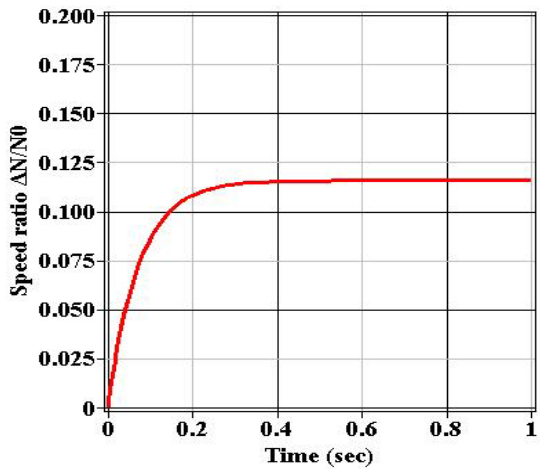


Fig. 7 Step response

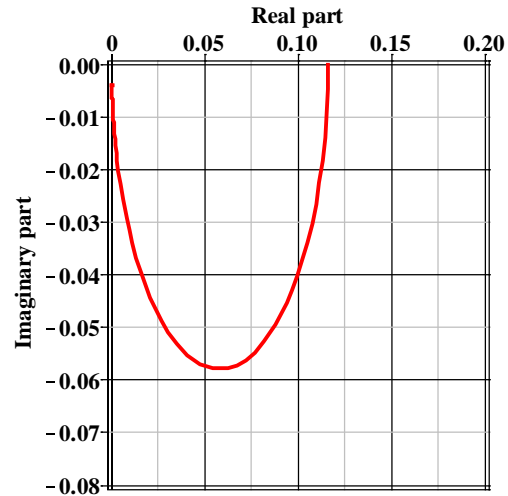


Fig. 8 Frequency response

The set of equations for the two-spool engine has the following form:

$$\begin{cases} (T^{(1)} \cdot s + \rho^{(1)}) \bar{N}_1 - k_{T_{41}}^{(1)} \bar{T}_{41}^* + k_{p_4}^{(1)} \bar{p}_4^* - k_{p_{41}}^{(1)} \bar{p}_{41}^* + k_{p_{21}}^{(1)} \bar{p}_{21}^* = 0 \\ (T^{(2)} \cdot s + \rho^{(2)}) \bar{N}_2 - k_{T_3}^{(2)} \bar{T}_3^* - k_{p_2}^{(2)} \bar{p}_2^* + k_{p_{21}}^{(2)} \bar{p}_{21}^* + k_{p_{41}}^{(2)} \bar{p}_{41}^* = 0 \\ \bar{T}_2^* - k_{p_2}^{(3)} \bar{p}_2^* + k_{p_{21}}^{(3)} \bar{p}_{21}^* = 0 \\ k_{n_1}^{(4)} \bar{N}_1 - k_{n_2}^{(4)} \bar{N}_2 + k_{p_{21}}^{(4)} \bar{p}_{21}^* - k_{p_2}^{(4)} \bar{p}_2^* = 0 \\ k_{p_{21}}^{(5)} \bar{p}_{21}^* + k_{n_2}^{(5)} \bar{N}_2 - k_{p_2}^{(5)} \bar{p}_2^* - k_{T_3}^{(5)} \bar{T}_3^* = 0 \\ \bar{T}_{41}^* - \bar{T}_3^* - k_{p_2}^{(6)} \bar{p}_2^* - k_{p_{41}}^{(6)} \bar{p}_{41}^* = 0 \\ \bar{T}_4^* - \bar{T}_{41}^* - k_{p_{41}}^{(7)} \bar{p}_{41}^* - k_{p_4}^{(7)} \bar{p}_4^* = 0 \\ k_{p_2}^{(8)} \bar{p}_2^* + k_{T_3}^{(8)} \bar{T}_3^* - k_{p_{41}}^{(8)} \bar{p}_{41}^* - k_{T_{41}}^{(8)} \bar{T}_{41}^* = 0 \\ k_{p_{41}}^{(9)} \bar{p}_{41}^* + k_{T_{41}}^{(9)} \bar{T}_{41}^* - k_{p_4}^{(9)} \bar{p}_4^* - k_{T_4}^{(9)} \bar{T}_4^* = k_{S_a}^{(9)} \bar{S}_a \\ k_{p_2}^{(10)} \bar{p}_2^* + k_{n_2}^{(10)} \bar{N}_2 + k_{p_{21}}^{(10)} \bar{p}_{21}^* + k_{T_3}^{(10)} \bar{T}_3^* - k_{T_2}^{(10)} \bar{T}_2^* = k_{W_f}^{(10)} \bar{W}_f \end{cases} \quad (19)$$

The transfer functions from the input variables fuel flow, $\bar{W}_f(s)$, and the exhaust nozzle area \bar{S}_a , to the output variable, LPC rotational speed $\bar{N}_1(s)$ and HPC rotational speed $\bar{N}_2(s)$, for a two-spool engine with

$$G_a = 90 \text{ kg/s}; T_3^* = 1500 \text{ K}; \pi_{C1} = 4; \pi_{C2} = 7; J_1 = 9.9 \text{ kg} \cdot \text{m}^2;$$

$$J_2 = 11.43 \text{ kg} \cdot \text{m}^2; N_1 = 9000 \text{ rot/min}; N_2 = 11000 \text{ rot/min};$$

are

$$\bar{N}_1(s) = \frac{(1.3s + 2.95)\bar{W}_f + (3.65s + 6.27)\bar{S}_a}{1.10s^2 + 4.99s + 5.60} \quad (20)$$

$$\bar{N}_2(s) = \frac{(2.51s + 5.87)\bar{W}_f - 3.32\bar{S}_a}{1.10s^2 + 4.99s + 5.60} \quad (21)$$

The responses of the rotational speeds $\bar{N}_1(t) = \Delta N_1 / N_1$ and $\bar{N}_2(t) = \Delta N_2 / N_2$ to an impulse input (Dirac function), to a unit step input (Heaviside function) and to a sinusoidal input ($s = i\omega$) for \bar{W}_f and \bar{S}_a are presented in Figures 9-17. Also, the temperature, velocity magnitude and velocity field in combustion chamber are presented in Figures 18-20.

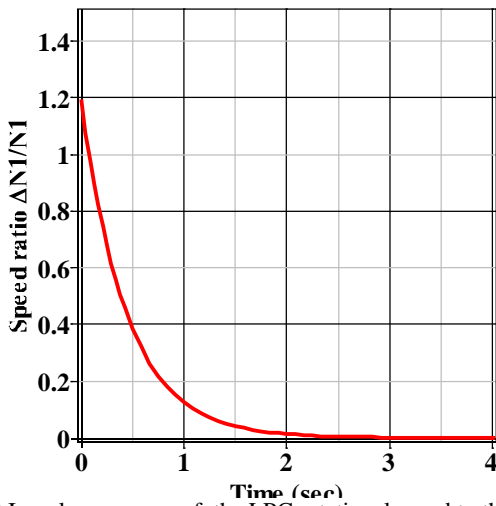


Fig. 9 Impulse response of the LPC rotational speed to the fuel flow rate input

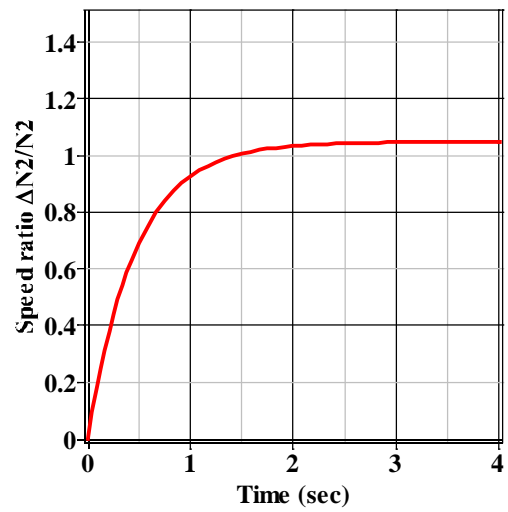


Fig. 12 Step response of the HPC rotational speed to the fuel flow rate input

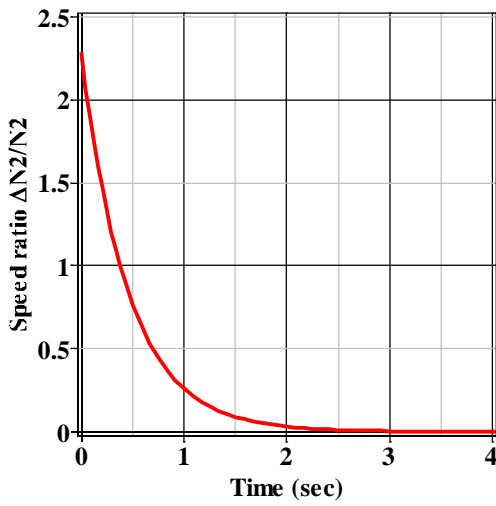


Fig. 10 Impulse response of the HPC rotational speed to the fuel flow rate input

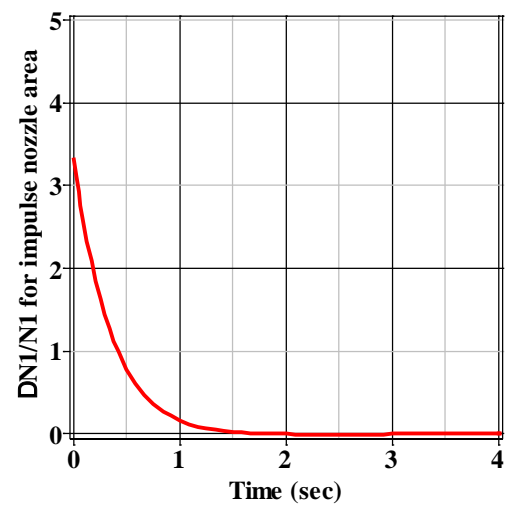


Fig. 13 Impulse response of the LPC rotational speed to the exhaust nozzle area input

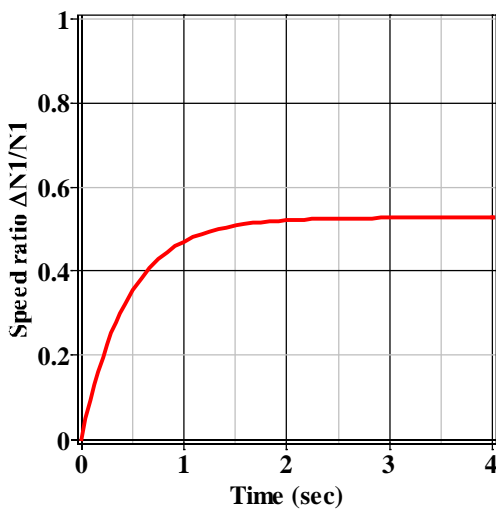


Fig. 11 Step response of the LPC rotational speed to the fuel flow rate input

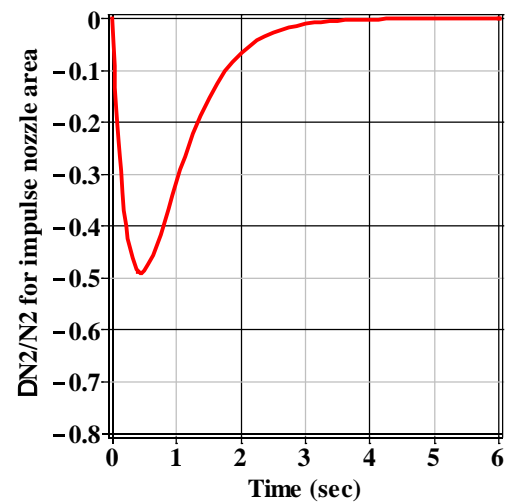


Fig. 14 Impulse response of the HPC rotational speed to the exhaust nozzle area input

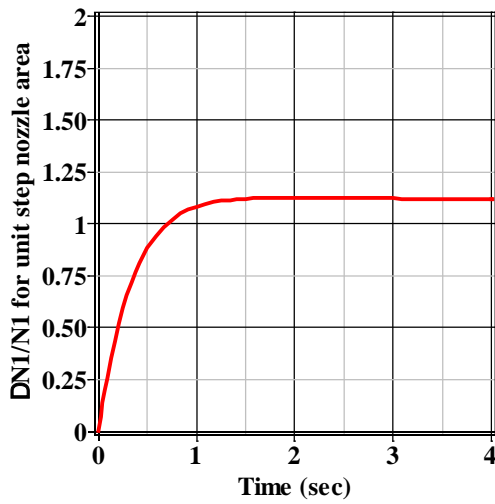


Fig. 15 Step response of the LPC rotational speed to the nozzle exhaust area input

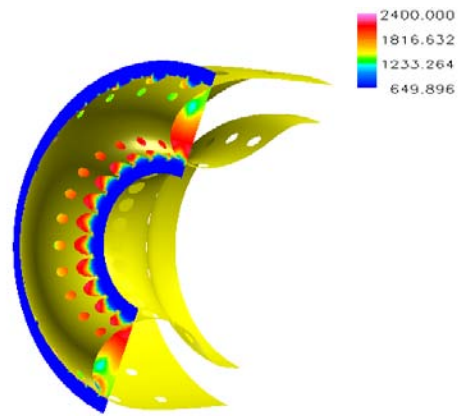


Fig. 18 Combustion chamber temperature

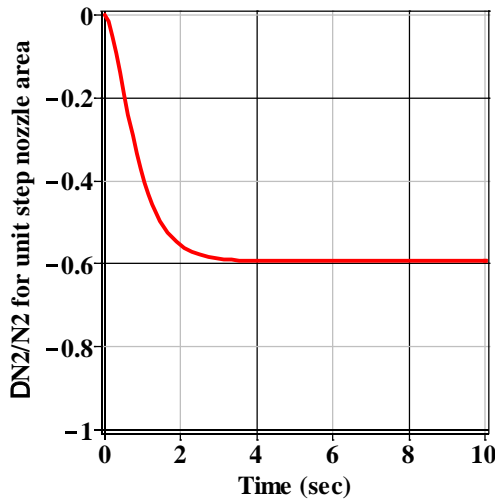


Fig. 16 Step response of the HPC rotational speed to the nozzle exhaust area input

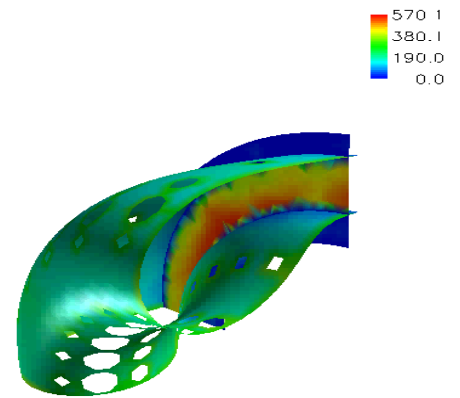


Fig. 19 Combustion chamber velocity magnitude

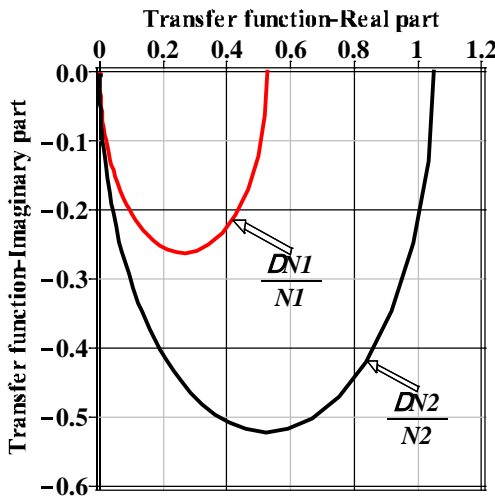


Fig. 17 Frequency response of the LPC and HPC rotational speed

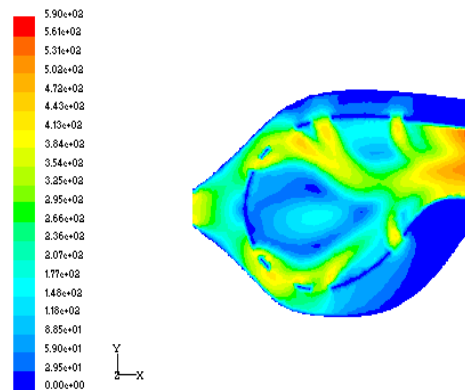


Fig. 20 Contour of velocity magnitude in combustion chamber

V. CONCLUSION

A low turbulence intensity environment in a fuel-air mixture flow of 50-100 m/s results in a root mean square of the turbulence fluctuation speed of 2.5-5 m/s. In a high turbulence intensity in a flow with a mean speed of 100 m/s, the turbulence contribution to flame propagation speed may be as high as 30 m/s.

The classical linear compensation is adequate only to govern the engine close to a fixed operating point, as defined by the current inlet conditions and desired thrust set point. Aside from nonlinearity and parametric changes in the engine, critical variables must be maintained within safety ranges. Linear compensation is the basic building block of standard aircraft engine control system. Parametric changes and nonlinearity are addressed with gain-scheduled linear compensators while limit protection logic schemes are used to override the active linear regulator when a critical variable approaches its safety limit. Even with constant control gains, limit relaxation is reflected in faster responses, and conversely, the main output response will become slower if limits are made more restrictive.

There are two ways of obtaining faster thrust response: redesigning the regulators for larger closed-loop bandwidths and relaxing the protective limits on variables which tend to peak as thrust response is made faster. Among the variables displaying such peaking are turbine outlet temperature, which peaks during acceleration, stall margin, which tends to undershoot during acceleration and combustor pressure, which tends to undershoot during deceleration.

In order to approach new constructive solutions for complex systems like the aircraft engines, it is necessary to use software codes to study the behavior or performances of these systems. For an aircraft engine the experimental validation is expensive, so the first step in this study is the simulation of the virtual model of constructive elements, like combustion chamber.

It is important to emphasize the inherent limitation in the use of the chemical reactor network approach in the simulation of combustion as the result of the simplification on the fluid mechanics equations, in contrast to the more elaborate description of the kinetic of combustion and the lower computational burden. A good alternative in the modeling and simulation of turbojet combustion systems could be the adoption of sophisticated approaches, such as the CFD, to get a better prediction of the thermodynamic performances of the turbojet combustion chambers.

NOMENCLATURE

The naming convention for the symbols representing engine models and control laws follows the convention defined as: T^* - total temperature [K]; p^* - total pressure [N/m^2]; π - pressure ratio; \dot{m} , G and W_f - mass flow rate [kg/s]; σ_{ca} - combustion chamber total pressure loss coefficient; γ - ratio of specific heat; $\gamma = 1.4$; $\gamma' = 1.33$; $\gamma_1 = (\gamma - 1)/\gamma$; c_p -

specific heat at constant pressure [$J/(kg \cdot K)$]; η - efficiency; HPC - high pressure compressor; LPC - low pressure compressor; $x_i = (x_i)_0 + \Delta x_i$; Subscripts: 0 - steady state; c - compressor; t - turbine; 1-5 engine cross section number; 2.1 - HPC inlet section; 4.1 - LPT inlet section.

REFERENCES

- [1] J. D. Mattingly, "Elements of Propulsion. Gas Turbines and Rockets", AIAA, Reston Virginia, USA, 2006.
- [2] L. C. Jaw, J. D. Mattingly, "Aircraft Engine Controls - Design, System Analysis and Health Monitoring", AIAA, Reston Virginia, USA, 2009.
- [3] S. Farokhi, "Aircraft Propulsion", John Wiley & Sons Inc., USA, 2009.
- [4] C. Rotaru, M. Mihaila-Andres, P. G. Matei, R. I. Edu, "Thermodynamic performances of the turbojet combustion chambers - numerical evaluation", Proceedings of the 2014 International Conference on Mechanics, Fluid Mechanics, Heat and Mass Transfer, ISBN 978-1-6184-220-0, pp. 86-91.
- [5] C. Rotaru, D. G. Safta, C. Barbu, "Aspects regarding internal flow in combustion chamber of turbojet engines", Proceedings of the 5th IASME/WSEAS International Conference on Fluid Dynamics and Aerodynamics, pp. 276-281, Greece, 2007.
- [6] R. F. Huang, H. F. Yang, C. M. Hsu, "Flame Behavior and Thermal Structure of Combusting Nonpulsating and Pulsating Plane Jets", Journal of Propulsion and Power, Volume 29, number 1, 2013, pag. 114-124.
- [7] R. D. Flack, "Fundamentals of Jet Propulsion with Applications", Cambridge University Press, 2005.
- [8] C. Rotaru, "Aspects Regarding Combustion Chamber Dynamics for Turbojet Engines", ICMT'09 International Conference on Military Technologies, Brno, Czech Republic, Proceedings, pag. 342-349, 2010.
- [9] J. D. Mattingly, W. H. Heiser, D. T. Pratt, "Aircraft Engine Design", second edition, AIAA, Reston Virginia, USA, 2002.
- [10] C. Rotaru, A. Arghiropol, C. Barbu, "Some aspects regarding possible improvements in the performances of the aircraft engines", Proceedings of the 6th IASME/WSEAS International Conference on Fluid Dynamics and Aerodynamics, pp. 196-201, Greece, 2008.